AIP | Journal of Applied Physics

Correlation between the spectroscopic and structural properties with the occupation of Eu3+ sites in powdered Eu3+-doped LiTaO3 prepared by the Pechini method

G. Gasparotto, M. A. Cebim, M. S. Goes, S. A. M. Lima, M. R. Davolos et al.

Citation: J. Appl. Phys. **106**, 063509 (2009); doi: 10.1063/1.3204967
View online: http://dx.doi.org/10.1063/1.3204967
View Table of Contents: http://jap.aip.org/resource/1/JAPIAU/v106/i6
Published by the AIP Publishing LLC.

Correlation between the spectroscopic and structural properties with the occupation of Eu^{3+} sites in powdered Eu^{3+}-doped $LiTaO_3$ prepared by the Pechini method

G. Gasparotto,[a] M. A. Cebim, M. S. Goes, S. A. M. Lima, M. R. Davolos, J. A. Varela, C. O. Paiva-Santos, and M. A. Zaghete
Instituto de Química, UNESP, São Paulo State University, Araraquara, São Paulo 14800-900, Brazil

(Received 18 March 2009; accepted 22 July 2009; published online 18 September 2009)

In this work we studied the structural and optical properties of lithium tantalate ($LiTaO_3$) powders doped with Eu^{3+} ions. We have examined the different sites occupied by the rare earth ion through the correlation of the DRX data analyzed with the Rietveld method and some spectroscopic parameters derived from the Eu^{3+} luminescence. A direct relation was established between the lattice parameters and the "occupation fraction" of Eu^{3+} in each $LiTaO_3$ site. The occupation fraction was set as the relative population of Eu^{3+} ions for each site obtained by means of the intensity, baricenter, and the spontaneous emission coefficients of the $^5D_0 \rightarrow {}^7F_0$ transitions. We concluded that the unit cell parameter *a* presents the same behavior of the Eu^{3+} occupation fraction in Ta^{5+} sites as a function of the Eu^{3+} content in $LiTaO_3$. The same was observed for the variation in Eu^{3+} occupation fraction in the Li^+ site and the unit cell parameter *c* with the Eu^{3+} content. © *2009 American Institute of Physics*. [doi:10.1063/1.3204967]

INTRODUCTION

Lithium niobate is a material endowed with interesting optical and electronic properties, which make it potentially applicable in optoelectronic devices.[1] Visible and infrared lasing properties can be obtained by doping $LiNbO_3$ with transition metals or trivalent lanthanides (Ln^{3+}).[2,3]

The optical and structural properties of Ln^{3+}-doped $LiNbO_3$ have been investigated by Liu *et al.*[4] Channeling techniques combined with Rutherford backscattering (RBS) or nuclear-reaction analysis (NRA) have become important tools for the analysis of impurities in the crystallographic lattice sites of metals[5,6] and semiconductors.[7,8]

The presence of impurities in such materials arises from the strong dependence of their spectroscopic properties on the chemical environment that surrounds the dopant. Ln^{3+} impurities when used as dopants in $LiNbO_3$ are incorporated with charge compensation, leading to the creation of defects.[9] Eu^{3+} is known by its unique optical properties and is considered a spectroscopic probe. However, in the case of $LiNbO_3:Eu^{3+}$, when its spectroscopic properties, i.e., spectral profile, are compared to the results of the channeling techniques, efforts to locate the crystallographic lattice site becomes largely ambiguous.[1]

Muñoz Santiuste *et al.*[10] studied the optical detection of Eu^{3+} sites in $LiNbO_3:Eu^{3+}$ and $LiNbO_3:MgO:Eu^{3+}$ crystals. Varing the [Li]/[Nb] molar ratio, it was concluded that Eu^{3+} replaces both Li^+ and Nb^{5+}, in at least four different chemical environments through the spectroscopic profile analysis of the Eu^{3+} $^5D_0 \rightarrow {}^7F_1$ intraconfigurational transition. Nonetheless Muñoz Santiuste *et al.* did also observe the evolution of Eu^{3+} concentration in each site with [Li]/[Nb] molar ratio.

Rebouta *et al.*[11] observed, using channel techniques with Monte Carlo simulation, that in $LiNbO_3:Eu^{3+}$, the dopant can occupy a crystallographic site varying within the range of 0.3–0.5 Å from the Li^+ site. Despite the distribution of Eu^{3+} in a single site, there is no mentioning of the nature and varieties of the chemical environments that surround it. Lithium tantalate ($LiTaO_3$) is very similar to $LiNbO_3$ not only because both are isostructural compounds but also due to the fact that Nb^{5+} and Ta^{5+} have the same ionic radius [0.74 Å; coordination number (CN)=6].[12]. In fact, because of the above mentioned features, $LiNbO_3:Eu^{3+}$ and $LiTaO_3:Eu^{3+}$ may have similar structural and spectroscopic properties. In a recent paper,[13] we did analyze the spectroscopy properties of $LiTaO_3:Eu^{3+}$ powder prepared by the Pechini method.[14] It was observed at least three Eu^{3+} sites without a center of symmetry, but no comments were advanced as to the nature of the sites as well as the relative amount of Eu^{3+} in each site.

In this work, we propose to use the spectroscopy properties of Eu^{3+} at different concentrations as a dopant in $LiTaO_3$ while correlating the results with the structural data obtained by the Rietveld method.[15]

EXPERIMENTAL PROCEDURE

The powdered $Li_{1+2x}Ta_{1-x}Eu_xO_3$ were prepared via the polymeric precursor method,[14] with $x=0.0010-0.0100$, similar to that described by Gasparotto *et al.*[13]

The x-ray diffraction data (XRD) were collected using a RIGAKU® RINT2000 rotating anode diffractometer with Cu $K\alpha$ radiation monochromatized by a curved graphite crystal, the interval lying between 20° and 100° (2θ), 0.02° (2θ) time per point of 0.3 s. The Rietveld refinement[15] was carried out using a GSAS (Ref. 16) suite with an EXPGUI (Ref. 17) interface. The peak profile function was modeled using a convolution of the Thompson–Cox–Hastings pseudo-Voigt

[a]Electronic mail: gisegasp@yahoo.com.br.

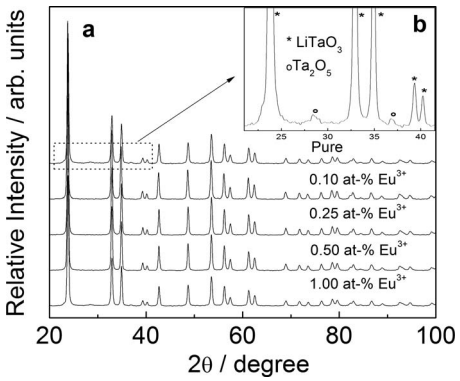

FIG. 1. XRD diffraction patterns of (a) pure lithium tantalate and doped lithium tantalate powders with different amounts of europium. (b) A close view showing a peak of secondary phase.

function,[18] as well as the asymmetry function described by Finger *et al.*[19] The model described by Larson and Von Dreele[16] was used to account for the anisotropy in the full width at half maximum (FWHM) reflections, while the model described by Stephens[20] was also used for anisotropic strain analysis.

The photoluminescence measurements were accomplished using spectroscopic excitation and emission from the solid powder samples at liquid nitrogen temperature (77 K). We have used a Fluorolog Spex F212L spectrofluorimeter, in the Front Face mode, a 450 W xenon lamp as the light source and a Hamamatsu R298 water cooled photomultiplier.

RESULTS AND DISCUSSION

Pure and doped crystalline lithium tantalate powders were obtained at 650 °C. Figure 1 shows some diffraction patterns of the pure $LiTaO_3$ and Eu-doped $LiTaO_3$, just as presented by the group in a recent published article.[13] The quantitative analysis of the phases based on the Rietveld method indicates a percentage of 1.1(1) wt % of Ta_2O_5 phase, which tells us that $LiTaO_3$ is present in 98.8(1) wt %. All the doped samples form a 100% $LiTaO_3$ phase, and this leads us to conclude that the presence of the Eu^{3+} ions reduces the temperature for the formation of the $LiTaO_3$ phase. Also, the doping ions are probably incorporated into the lattice of $LiTaO_3$ once no secondary phases have been detected taking into account the limit of detection.

As a luminescent probe of crystallographic sites and symmetry of RE^{3+} ions in the $LiNbO_3$ host, Eu^{3+} ion has been used as a dopant because its specific emission properties and nonsplitted $^5D_0 \rightarrow {}^7F_0$ transition. Four sites have been found for Eu^{3+} in $LiNbO_3$ structure by the analysis of time resolved and site selective measurements.[10,21] The formation of Eu^{3+} $(Nb^{5+})-Eu^{3+}(Li^+)$ pairs has been suggested for the major Eu(3) and Eu(4) sites, while Eu^{3+}(1,2) ions in Nb^{5+} lattice positions.

The emission spectra of Eu^{3+}-doped $LiTaO_3$ samples in the spectral region of 575–587 nm are presented in Fig. 2. The excitation was performed in the $Eu^{3+}-O^{2-}$ charge transfer band (270 nm). In this region, the Eu^{3+} $^5D_0 \rightarrow {}^7F_0$ (0-0) transitions were observed. For this transition, since $J=0$, no splinting patterns are expected for the $^5D_0$ and $^7F_0$ levels.

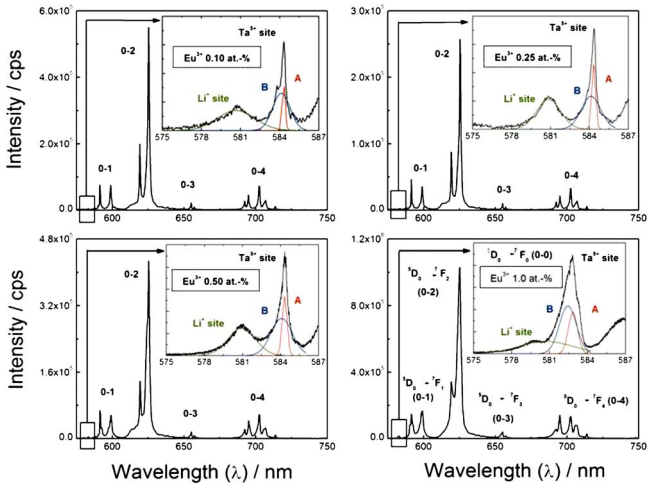

FIG. 2. Emission spectra of LiTaO3 : Eu^{3+} samples. The excitation was fixed at the $Eu^{3+}-O^{2-}$ charge transfer band. The band deconvolution is presented as doted lines and the band assignment is made in the spectrum.

Therefore, the number of observed bands assigned to this transition corresponds directly to the number of Eu^{3+} sites without an inversion center.

In the emission spectra of Fig. 2, two sets of bands are highly noticeable: one of those centered at 581 nm and the other one at about 584 nm. In the primer, only one band that reveals just one site can be observed. The former set of 0-0 bands can be ascribed to at least two sites. The deconvolution of the 0-0 bands are also shown in Fig. 2, presented as doted lines under the continuous lines representing the original spectra, where we use Gaussian bands to perform the fitting process. The assignment of each band was presented in accordance with the sites of $LiTaO_3$. In this compound three distorted octahedral sites (CN=6) were available, i.e., the Li^+ site, the Ta^{5+} site, and a free octahedral site. We ascribed the 0-0 band at 581 nm to a Eu^{3+} ion occupying a Li^+ site, while the set of 0-0 bands around 584 nm was ascribed to a Eu^{3+} ion at a Ta^{5+} site.[13] Due to the proximity of the two bands centered at 584 nm, that is, a small $\Delta\lambda$ ($\sim$0.30 nm) between 584 nm bands as compared to the $\Delta\lambda$ ($\sim$3.0 nm) between the two sets of 0-0 bands (581/584 nm), both were ascribed to a Eu^{3+} at a Ta^{5+} site. The 584 nm bands were named A and B, respectively.

Let us now consider the intensity (I) of the 0-0 transition. This quantity is proportional to the area (S) under the spectral band and depends explicitly on the Einstein spontaneous emission coefficient (A_{rad}) of the said transition, its baricenter (ω), and the population (N) of Eu^{3+} ions in the excited state ($^5D_0$), and this expression can be written as[22,23]

$$I = h\omega N A_{rad} = S. \quad (1)$$

Since all sites of the $LiTaO_3$ matrix are distorted octahedrals, there are two possible approximations to consider. First let set the spontaneous emission coefficients (A_{rad}) and the baricenter (ω) of the 0-0 bands as having approximately the same value. Therefore, the occupation fraction of a given Eu^{3+} site (F_i) will be proportional to the ratio of its corresponding 0-0 band area (S_i) and the total area of the 0-0 bands ($\Sigma_i S_i$), i.e.,

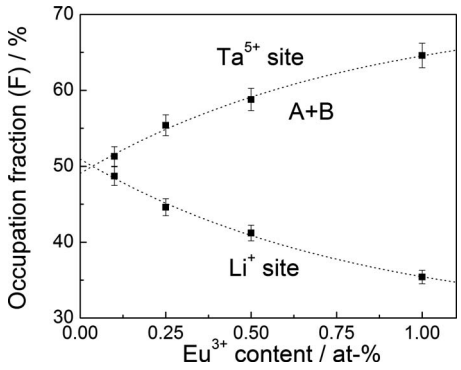

FIG. 3. Occupation fraction of Eu^{3+} sites in LiTaO3 as a function of the Eu^{3+} amount in mol %. The set of bands centered at 584 nm was assigned to a vacant Ta^{5+} site and the occupation fraction is the sum of F for sites A and B.

$$F_i = \frac{N_i}{\Sigma_i N_i} = \frac{S_i}{\Sigma_i S_i}. \tag{2}$$

By taking into account the area under the 0-0 bands observed in the emission spectra of $LiTaO_3:Eu^{3+}$ samples, it was possible to determine the occupation fraction of Eu^{3+} ions in the sites of the $LiTaO_3$ matrix. Now, if only the spontaneous emission coefficients were considered equal, we have to change S_i by $\tilde{S}_i$ which is the ratio S_i/ω_i, and instead of having the occupation fraction F, we will get $\tilde{F}$. In practice, as our first subjection is reliable, both occupation fractions (F and $\tilde{F}$) do not have significant changes in their values and they have the same behavior as a function of the Eu^{3+} content. For that reason and in order to simplify the discussion, we will only deal with F. The occupation fraction of Eu^{3+} ions are presented in Fig. 3.

The general tendency observed in F as the Eu^{3+} content increases from 0.10 to 1.00 at. % is that there is an increase in the amount of substitutions in Ta^{5+} sites (A and B), followed by a diminution of substitutions in the Li^+ site. The magnitude of F, the position of the 0-0 band in the emission spectrum, and the FWHM for each site are presented in Table I. The position of the bands has small shifts, and all bands are relatively broad, with a FWHM=15 cm^{-1}, a characteristic that justifies the Gaussian shape of each 0-0 emission.[10] The results are compatible with the work of Muñoz Santiuste *et al.*,[10] which correlated the $^5D_0 \rightarrow {}^7F_1$ (0-1) emission area of Eu^{3+} with the [Li]/[Nb] molar ratio in $LiNbO_3:Eu^{3+}$ 1.0 at. % crystals. Muñoz Santiuste *et al.* described a total of four sites which were divided into two sets: the first one has an increase in the 0-1 emission area with an increasing [Li]/[Nb] molar ratio, while the second recorded a decrease in the 0-1 emission area. Thus, this leads us to deduce that the same distribution pattern of Eu^{3+} ions is observed once the [Li]/[Nb] molar ratio is varied in $LiNbO_3:Eu^{3+}$ 1.0 at. % and with a fixed [Li]/[Ta]=1 ratio and a variable Eu^{3+} content.

More so, for a description of the general tendency observable in the occupation fraction in Fig. 3, we first considered the difference in the ionic radii for Li^+, Ta^{5+}, and Eu^{3+}. In a chemical environment with CN=6, Li^+ has an ionic radius of 0.76 Å, while Ta^{5+} has an ionic radius of 0.64 Å (Ref. 12). Both ions have a large difference when compared to Eu^{3+}, which has an ionic radius of 0.943 Å (Ref. 12). However, taking into account only this parameter, there is a considerable preference for the substitution of Li^+ ions. In the same light, if the charges of the ions were considered, then the Eu^{3+} ions might substitute Ta^{5+} ions since tantalum possesses a higher charge. Both aspects are important for the vivid description of the formation of the $LiTaO_3:Eu^{3+}$ solid solution; however, the importance of each effect can only be well understood once the Eu^{3+} incorporation reactions in the $LiTaO_3$ matrix as well as the defects created in this process are known.

The substitution of a Li^+ ion by a Eu^{3+} may be represented by the incorporation of $EuTaO_4$ into $LiTaO_3$, hence forming a solid solution as can be seen below,

$$EuTaO_4 \xrightarrow{LiTaO_3} Eu_{Li}^{**} + Ta_{Ta}^{\times} + O_I'' + O_o^{\times}. \tag{3}$$

where interstitial oxygens (O_I'') are formed. Alternatively, if a Eu^{3+} ion substitutes a Ta^{5+} ion, one might consider the incorporation of $LiEuO_2$ into $LiTaO_3$, hence forming once again a solid solution indicated as follows:

$$LiEuO_2 \xrightarrow{LiTaO_3} Li_{Li}^{\times} + Eu_{Ta}'' + V_o^{**} + O_o^{\times}, \tag{4}$$

where oxygen vacancies (V_O^{**}) are formed. Finally, with a Eu^{3+} ion occupying the vacant site, the incorporation will create interstitial oxygens (O_I'') as well as cation vacancies (V_{Li}' or $V_{Ta}^{5'}$).

TABLE I. Baricenter (nm), FWHM (cm^{-1}) of the 0-0 bands, and occupation fraction of Eu^{3+} in each $LiTaO_3$ sites. For the Ta^{5+} site, F_1 is presented as the occupation fraction of sites A, B, and A+B, respectively.

	Ta^{5+} site			Li^+ site		
Eu^{3+} content (at. %)	F_1 (%)	$^5D_0 \rightarrow {}^7F_0$ (nm)	FWHM ($^5D_0 \rightarrow {}^7F_0$) ($cm^{-1}$)	F_2 (%)	$^5D_0 \rightarrow {}^7F_0$ (nm)	FWHM ($^5D_0 \rightarrow {}^7F_0$) ($cm^{-1}$)
0.10	42.0/9.32 51.3	584.31/584.13	13.00/78.24	48.7	580.65	172.15
0.25	15.5/39.9 55.4	584.32/584.12	17.57/87.76	44.6	580.85	109.79
0.50	15.7/43.1 58.8	584.33/584.10	22.25/98.37	41.2	580.94	128.95
1.00	20.7/44.0 64.6	582.85/582.45	39.7/79.31	35.4	580.74	248.68

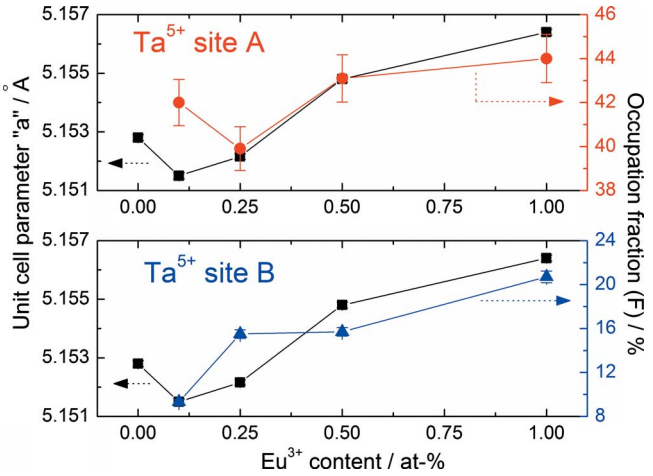

FIG. 4. (Color online) Variation in the unit cell parameter for the vacant Ta^{5+} sites A and B as a function of the Eu^{3+} amount along with the variation in the occupation fraction of each site. The variation in the unit cell parameter is presented in the left side of the *y* axis, while the occupation fraction is presented in the right side.

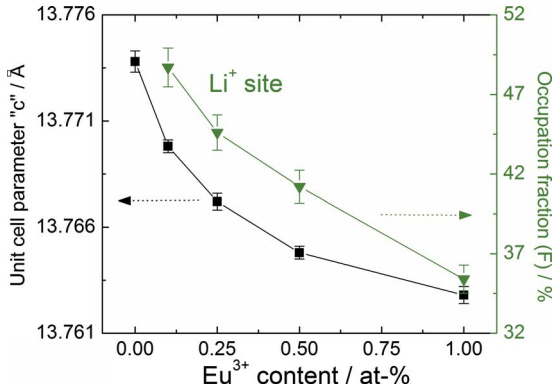

FIG. 5. (Color online) Variation in the unit cell parameter *c* and occupation of the vacant Li^+ site as a function of the Eu^{3+} amount. The variation in the unit cell parameter is presented in the left side of the *y* axis, while the occupation fraction is presented in the right side.

The Eu^{3+} incorporation into a Li^+ site as suggested in Eq. (3) creates interstitial oxygens (O_I''), which, in an opened structure, may have a small enthalpy of formation; on the other hand, this defect tends to increase the Eu^{3+} CN, resulting in an increase in its atomic radius. The said effect will be unfavorable for the substitution of Li^+. In the case of a Ta^{5+} substitution, as suggested in Eq. (4), the formation of oxygen vacancies tends to be favorable because this same defect leads to the formation of a more opened structure, with a small enthalpy of formation. Consequently, the incorporation of Eu^{3+} ions into Ta^{5+} sites tends to prevail. Moreover, this effect will be more evidenced where there is an increase in the Eu^{3+} content. Nevertheless, the formation of oxygen vacancies is more favorable once it gives rise to opened local structures, which can easily incorporate Eu^{3+} ions that possesses the highest ionic radius compared to Li^+ and Ta^{5+}.

The results found for the occupation fraction of the three observed sites as a function of the Eu^{3+} content were compared as well as the variation in the unit cell parameters and the molar volume, both derived by the Rietveld refinement of the XRD data. In Fig. 4 the occupation fraction of the Ta^{5+} sites is compared with the variation in the *a* cell parameter as a function of the Eu^{3+} content. The red line stands for the Ta^{5+}(A) site, whereas the blue one for the Ta^{5+}(B) site. The behavior of the occupation fraction curves is similar to the variation in the *a* unit cell parameter, bearing an increase in both quantities with the Eu^{3+} content. Some deviations can though be observed in the occupation fraction of the Ta^{5+}(A) site of $LiTaO_3:Eu^{3+}$ 0.10 at. % as well as in the Ta^{5+}(B) site of $LiTaO_3:Eu^{3+}$ 0.25 at. %. Besides, the sum of the two occupation fractions of Ta^{5+} sites (A+B) gives us the total *F* as presented in Fig. 3.

For the Li^+ site, the behavior of the occupation fraction as a function of the Eu^{3+} content is similar to that presented in Fig. 3, although the comparison between the variation in the *c* unit cell parameter with the Eu^{3+} content is exactly the same (Fig. 5). As the $F(Li^+)$ diminishes with the Eu^{3+} content, the unit cell volume (*V*) will strongly depend on the $F(Ta^{5+})$, which thus lead to a similar variation in *V* and *a* as a function of the Eu^{3+} content.

CONCLUSION

We have reported the distribution and occupation fraction (*F*) of $LiTaO_3$ sites by Eu^{3+} ions and correlated the results with the Rietveld analysis of XDR data. The pure and Eu^{3+}-doped $LiTaO_3$ were prepared by the Pechini method with a firing temperature of 650 °C. The spectral pattern of the $^5D_0 \rightarrow {}^7F_0$ (0-0) transition were analyzed, and each 0-0 band was fitted to a Gaussian function, the area of the band was then correlated with the population of Eu^{3+} ions. It was observed that the Eu^{3+} substitutes Li^+ and Ta^{5+}, with a preference over the occupation of Ta^{5+} sites, which have an increasing Eu^{3+} concentration. The above observation was arrived at due to the formation of oxygen vacancies (V_O^{**}), and once Eu^{3+} substitutes a Ta^{5+} ion, this leads to more opened structures that can more easily accommodate an ion with large ionic radius compared to Ta^{5+} or Li^+. Interestingly, we notice that when Eu^{3+} occupies a Li^+ site instead of substituting a Ta^{5+} ion, interstitial oxygens (O_I'') are formed to compensate the total charge. The formation of this defect increases the Eu^{3+} CN and, consequently, its ionic radius. Additionally, we correlated the variation in the occupation fraction of each site with the variation in the unit cell parameters by the Rietveld analysis method. By so doing, we could observe variations in the unit cell parameters similar to that observed in the occupation fraction with Eu^{3+} concentration.

[1]A. Lorenzo, H. Jaffrezic, B. Roux, G. Boulon, and J. García-Solé, Appl. Phys. Lett. **67**, 3735 (1995).
[2]L. F. Johnson and A. A. Ballman, J. Appl. Phys. **40**, 297 (1969).
[3]W. Ryba-Romanowski, I. Sokólska, G. Dominiak-Dzik, and S. Golab, J. Alloys Compd. **300–301**, 152 (2000).
[4]M. Liu, D. Xue, and K. Li, J. Alloys Compd. **449**, 28 (2008).
[5]R. Vianden, E. N. Kaufmann, and J. W. Rodgers, Phys. Rev. B **22**, 63 (1980).
[6]W. Segeth, D. O. Boerma, L. Niesen, and P. J. M. Smulders, Phys. Rev. B **39**, 10725 (1989).
[7]B. Bech Nielsen, Phys. Rev. B **37**, 6353 (1988).
[8]P. J. Smulders, D. O. Boerma, B. Bech Nielsen, and M. L. Swanson, Nucl. Instrum. Methods Phys. Res. B **45**, 438 (1990).
[9]H. Donnerberg, S. M. Tomlinson, C. R. A. Catlow, and O. F. Schirmer,

Phys. Rev. B **44**, 4877 (1991).
[10]J. E. Muñoz Santiuste, B. Macalik, and J. García Solé, Phys. Rev. B **47**, 88 (1993).
[11]L. Rebouta, J. C. Soares, M. F. da Silva, J. A. Sanz-García, E. Diéguez, and F. Aguiló-Lopez, Appl. Phys. Lett. **55**, 120 (1989).
[12]R. D. Shannon, Acta Crystallogr., Sect. A: Cryst. Phys., Diffr., Theor. Gen. Crystallogr. **32**, 751 (1976).
[13]G. Gasparotto, S. A. M. Lima, M. R. Davolos, J. A. Varela, E. Longo, and M. A. Zaghete, J. Lumin. **128**, 1606 (2008).
[14]M. P. Pechini, U.S. Patent No. 3,330 (1967) 69.
[15]H. M. Rietveld, J. Appl. Crystallogr. **2**, 65 (1969).
[16]C. Larson, R. B. Von Dreele, Los Alamos National Laboratory Report No. LAUR 86, 2000.
[17]B. H. Toby, J. Appl. Crystallogr. **105**, 210 (2001).
[18]R. A. Young and P. Desai, Arch. Nauki Mater. **10**, 71 (1989).
[19]L. W. Finger, D. E. Cox, and A. P. Jephcoat, J. Appl. Crystallogr. **27**, 892 (1994).
[20]P. Stephens, J. Appl. Crystallogr. **32**, 281 (1991).
[21]D. Hreniak, A. Speghini, M. Bettinelli, and W. Strek, J. Lumin. **119**, 219 (2006).
[22]O. L. Malta, H. F. Brito, J. F. S. Menezes, F. R. Gonçalvez e Silva, S. Alvez, Jr., F. S. Farias, Jr., and A. V. M. de Andrade, J. Lumin. **75**, 255 (1997).
[23]F. A. Sigoli, H. F. Brito, M. Jafelicci, Jr., and M. R. Davolos, Int. J. Inorg. Mater. **3**, 755 (2001).